Pergamon

PII: S0043-1354(97)00233-9

Wat. Res. Vol. 32, No. 3, pp. 905–914, 1998

Printed in Great Britain
0043-1354/98 $19.00 + 0.00

TERNARY EXPRESSION STAGE IN BIOLOGICAL SLUDGE DEWATERING

I. L. CHANG[1] and D. J. LEE[1]*

[1]Department of Chemical Engineering, National Taiwan University, Taipei, Taiwan 106, R.O.C.

(First received December 1996; accepted in revised form June 1997)

Abstract—The expression characteristics of original and freeze/thaw conditioned waste activated sludges were experimentally evaluated. Results in this study indicate that the first two stages of expression (primary and secondary consolidation) are similar to those of a particulate system, on which the model analysis by Shirato *et al.* (1974) is applicable. In the final phase of the expression of biological sludge, however, an unexpected constant-rate consolidation period, termed herein the ternary consolidation period, is observed. A modified combined Terzaghi-Voigt rheological model is proposed to describe the relation between void ratio and compressive pressure of the sludge cake. Whereas the resulting governing equation is solved analytically and the model parameters are found by regression analysis. The ternary consolidation is speculated to arise from the erosion of strongly bound moisture from the biological particles. © 1998 Elsevier Science Ltd. All rights reserved

Key words—expression, activated sludges, ternary consolidation, freeze/thaw treatment, modeling

NOMENCLATURE

- A parameter defined in equation (A2), m^{-1}
- a_c compressibility coefficient of secondary consolidation defined as $(1 + e)/E_2$, Pa^{-1}
- a_E compressibility coefficient of primary consolidation defined as $(1 + e)/E_1$, Pa^{-1}
- a_G compressibility coefficient of ternary consolidation defined as $(1 + e)/G_3$, $Pa^{-1}s^{-1}$
- B the ratio of secondary consolidation to the total consolidation, -
- C_e modified consolidation coefficient based on specific solid volume, (m^2/s)
- D_{1n} parameter defined in equation (A14), -
- D_{2n} parameters defined in equation (A15), -
- E_1 rigidity of Terzaghi element, Pa
- E_2 rigidity of Voigt element, Pa
- e local void ratio, -
- e_1 initial void ratio, -
- F parameter defined as $F = i\gamma\theta_c^*/K$, -
- G_2 viscosity of Voigt element of secondary consolidation, Pa-s
- G_3 viscosity of Voigt element of ternary consolidation, Pa-s
- i number of drainage surfaces, -
- K parameter defined as $K = 1 + \beta + i\gamma\theta_c^*$, -
- L cake thickness, m
- L_1 initial cake thickness, m
- L_f final cake thickness, m
- P applied pressure, Pa
- P_S local solid compressive pressure, Pa
- P_{Si} local solid compressive pressure of material at beginning of consolidation, Pa
- $q(s)$ function defined in equation (A9), s^{-1}
- $r(s)$ function defined in equation (A8), s^{-1}
- S_3 shear strain of the dashpot, -
- s variable of Laplace transform, s^{-1}
- U_c consolidation ratio, -
- u local apparent relative velocity of liquid to solid, m/s
- α_{av} average specific resistance of cake, m/kg
- β parameter defined as a_C/a_E, -
- γ parameter defined as $\gamma = a_G/a_E$, s^{-1}
- λ root for $q(s) = 0$ as defined in equation (A12), s^{-1}
- η creep constant defined by $\eta = E_2/G_2$, s^{-1}
- τ variable of Laplace transform, s
- θ_c consolidation time, s
- θ_C^* the end of consolidation time, s
- μ viscosity of liquid, Pa-s
- ρ_S true density of solid, kg/m^3
- ω variable of indicating an arbitrary position in cake, m
- ω_0 total solid volume in cake per unit sectional area, m
- ξ dummy variable, m

*Corresponding author. Fax: 886-2-362-3040, e-mail: djlee@ccms.ntu.edu.tw.

INTRODUCTION

Owing to the relatively low energy consumption rate involved, compared with the thermal dewatering methods, expression by mechanical pressure is widely employed in industries to separate liquid from a cake (Tiller and Yeh, 1987).

In recent decades, most research works on expression has been undertaken by Japanese researchers Shirato and Murase. In 1965, they employed the Terzaghi spring analogy to analyze the constant pressure expression process from which they obtained a simple analytical solution for primary consolidation. In 1974, to incorporate the creep effect in consolidation process, Shirato *et al.* (1974) adopted the Voigt element in modeling the secondary consolidation and obtained a complicated solution for the combined Terzaghi-Voigt model with three parameters (B, η, and Ce). B and η represent respectively the fraction of the secondary consolidation to the overall consolidation and the ratio of the rigidity and the viscosity of the Voigt model. The coefficient of consolidation, the Ce value, accounts for the combined effect for cake specific resistance and the primary consolidation period.

(Note: the combined Terzaghi-Voigt model is a phenomenological model that lacks theoretical basis. The spring element in Terzaghi model accounts for the elastic behavior of cake, whose action under loading is referred to as the "primary consolidation". The dashpot and spring elements in the Voigt model account for the viscous behavior, whose action under loading is referred to as the "secondary consolidation".)

At infinite expression time limit and assuming that the viscosity of the dashpot in the Voigt model is much larger than the spring rigidities, the following simple asymptotic solution is obtained:

$$U_c = 1 - B\exp(-\eta\theta_c). \quad (1)$$

where U_c is the consolidation ratio defined as $(L_1 - L)/(L_1 - L_f)$, L is the cake thickness at consolidation time θ_c and L_1 and L_f are the initial and equilibrium cake thickness, respectively.

Equation 1 is found to be effective with several common particulate systems, such as kaolin or clay slurries (Chang *et al.*, 1997a, b). The corresponding B and η coefficients were determined (Shirato *et al.*, 1977, 1978, 1979). The third parameter Ce can be estimated by a graphical method (Shirato *et al.*, 1970).

Many expression applications are devoted to the mechanical dewatering of biological sludge cakes (Vesilind, 1979). Several distinct features make the biological sludge systems very different from conventional particulate systems. For example, the highly porous, fractal-like floc interior structure (Li and Ganczarczyk, 1989, 1990), the high resistance to dewatering (Chen *et al.*, 1996a), and a large amount of so-called "bound water" (Vesilind, 1994). The bound water content has been observed to correlate strongly with the performances of many sludge processes (Drost-Hansen, 1977, Katsiris and Kouzeli-Katsiri, 1987, Robinson and Knocke, 1992). The use of an expression for estimating bound water content in sludge has been recently reported (Lee, 1994a; Lee and Hsu, 1994, 1995; Lee and Lee, 1995; Chen *et al.*, 1997). Kawasaki *et al.* (1990, 1994) provided the first experimental and theoretical study on biological sludge expression. They concluded that, except in the final phase of expression ($U_c > 0.8$), the conventional Terzaghi-Voigt type analysis originally proposed for inorganic sludges is equally applicable to their biosludges.

In this paper, we perform an experimental investigation of the constant-pressure expression of activated sludges, original and freeze/thaw conditioned. Because of the discrepancy suggested by Kawasaki *et al.* (1990, 1994) between the traditional combined Terzaghi-Voigt model and the experiments, a modified rheological model incorporating the bound water erosion mechanism is proposed and the resulting expression equation is solved analytically. A form of asymptotic solution is derived from which the model parameters are estimated and interpretation given.

EXPERIMENTAL

Activated sludge samples taken from Neili Bread Plant, Presidential Enterprise, Taoyuan, Taiwan were tested within two hours after sampling. The COD and SS data of the supernatant drawn from the sludge, measured via EPA Standard Methods, were 18.8 and 1.0 mg/L, respectively. The weight percentage of dried solid content measured 0.6% (w/w). In another independent sludge test employing sludge sediment, the corresponding weight percentage is 1.7% (w/w).

Freeze/thaw conditioning is an efficient method of changing floc structure and reducing the bound water content in sludge (Lee and Hsu, 1994). We employed the same in the present work to investigate the effects of such physical conditioning on the corresponding expression characteristics change. The sample is placed in a stainless steel vessel measuring 25 cm in diameter, 0.15 cm thick and 25 cm high. The vessel is immersed for 48 h in a freezing pool at a temperature of -15°C. Both the upper and lower surfaces of the sample chamber are insulated, with the result that the direction of heat transfer (the direction of ice formation/migration) is along the radial direction. Kawasaki and Matsuda (1993) have defined an average freezing speed as the ratio between the radius of the sample chamber and the time required for complete freezing. The resulting average freezing speed is around 0.71 μm/s. The frozen sample was then thawed for 24 h at room temperature. The freeze/thaw conditioned sludge is hereinafter referred to as the "conditioned sludge". The weight percentage of the conditioned sludge sample was 0.7% (w/w). True solid density data for the original and conditioned sludges, measured by Accupyc Pycnometer 1330 (Micrometritics), were all approximately 1450 kg/m^3. The particle size distribution (PSD) was determined by a Particle Sizer (Coulter LS230). The mean floc diameters for the original and the conditioned sludges are 130 and 440 μm, respectively. The floc shape, observed by microphotographs (Micromeritics), is a fractal-like, loose aggregate. After the freeze/thaw treatment, the flocs are round shaped with a more compact structure. The microphotographic observations are similar to those in Hung *et al.* (1996) and, for brevity's sake, are not shown here. Notably, these flocs are highly fragile and largely tend to break down during filtration and consolidation. The correlation between the floc size and shape information and the sludge expression characteristics is therefore unclear.

Biological sludge during long time storage or expression decomposes. Testing of original sludge is accomplished within 2 (transportation) h + 2 to 4 (expression test) h, a far shorter time period than that spent in Kawasaki *et al.* (1990, 1994) (up to 44 h) and is one that has apparently negligible effects on sludge characteristics.

For comparison, kaolin powders and clay powders served as the particulate testing materials. Their particle size distribution was determined by Sedigraph 5100C (Micromeritics), with an addition of 0.5% w/w dispersant (Darvan C, R. T. Vanderbuilt, Norwalk, CT) to maintain the particles in a dispersed state. The distribution was monodispersed and the mean particle diameter for the kaolin and clay samples were approximately 2.3 μm and 4.5 μm, respectively. With a relative standard deviation of less than 0.5%, true solid density was measured by a pycometer. The true density for kaolin was 2727 kg/m^3 , and for clay, 2584 kg/m^3. The weight percentages for kaolin and clay slurries were at 20% (w/w). A mercury penetration test demonstrated that both particulate samples were basically nonporous.

A constant head piston press (Triton Electronics, type 147) was employed for all the expression tests. The testing sludge (375 g for clay and kaolin tests and 350 g for sludge tests) was placed in the inner stainless steel cylinder measuring 7.62 cm in diameter, 20 cm high and covered with a movable piston. A hydraulic pressure of 1000 psi was then exerted on the piston to force the moisture out through the lower drainage surface. The time evolution of the filtrate weight was automatically recorded by an electronic balance connected to a personal computer. The residual moisture content of the cake in equilibrium with the applied pressure was determined by weighing and drying at the end of expression. This residual moisture may include some physically adsorbed and most of the chemically bounded water content (Lee and Hsu, 1995).

Having the filtrate weight versus time data, and the information about the solid content and true solid density, the porosity of cake can be subsequently obtained. Notably, the bound water of a sludge would move together with and should be considered a part of the solid phase (Michaels and Bolger, 1962; Kawasaki *et al*., 1991; Lee, 1994b). Since the biological particles are highly deformable, almost all the mechanically removable moisture is exhausted on entering the equilibrium stage (Lee and Hsu, 1995). Assuming that the residual moisture after expression is the bound water of the sludge (Lee, 1994a), and that the bound water is a part of the particle phase, the final porosity of the cake (free water/(free water + true solid + bound water)) should therefore be zero. However, under varying compressive pressures the residual moisture remained in the cake will be different as well. Such an interpretation of porosity leaves some ambiguity. Nevertheless, employing this definition of porosity will only shift the expression curves downwards. Such a shift will not influence the subsequent discussions on the model parameters. The porosity curves shown in the subsequent sections (Fig. 1) should serve for demonstration purpose only. Direct comparison among the curves are not strictly meaningful.

RESULTS AND DISCUSSION

General

Figure 1 illustrates typical expression curves. A complete test actually consists of two stages: the filtration stage and the consolidation stage, denoted by the symbols F and C in the figure. Shirato *et al*. (1967) proposed a simple graphical method for locating the transition point between the two stages. Yeh (1985) employed an alternative method: a certain amount of gas was retained in the expression chamber and this was then forced out through the cake once the piston touched the cake surface. We herein adopted Shirato's method, since the transition point can be easily determined graphically. The obtained transition points are indicated by the arrows in Fig. 1.

The expression stage can thereby be differentiated from the filtration stage and is redrawn in Fig. 2. The curve for the original activated sludge is the farthest right one of all curves, indicating a much higher resistance to expression dewatering. This phenomenon is also commonly found for other biological sludges (Lee, 1994b; Lee and Lee, 1995). Freeze/thaw conditioning is found to significantly enhance the efficiency of the filtration stage (ranking first in the filtration stage), and to mildly enhance expression efficiency (ranking third in the expression stage). However, in this work we focus only on the expression stage. Interestingly, in activated sludge experiments, the moisture removal rate after a characteristics expression time θ_c^* suddenly drops. This occurrence caused the porosity curve to apparently intercept the line of zero porosity at sharp angles. A rather rapid transition occurs close to the zero porosity axis.

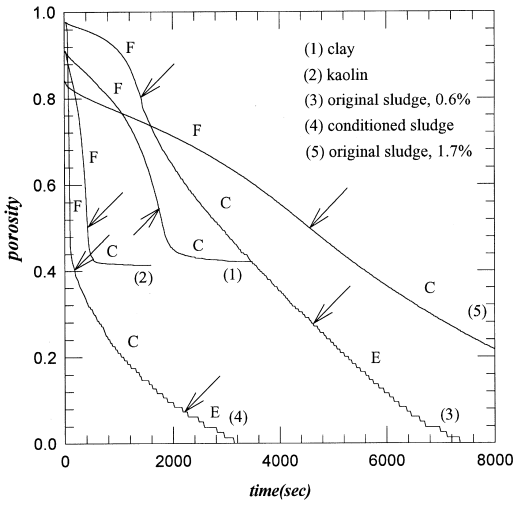

Fig. 1. Cake porosity versus time plot. P = 1000 psi. F: filtration stage; C: consolidation stage; E: final constant-rate period. Arrows indicate the transition points among stages.

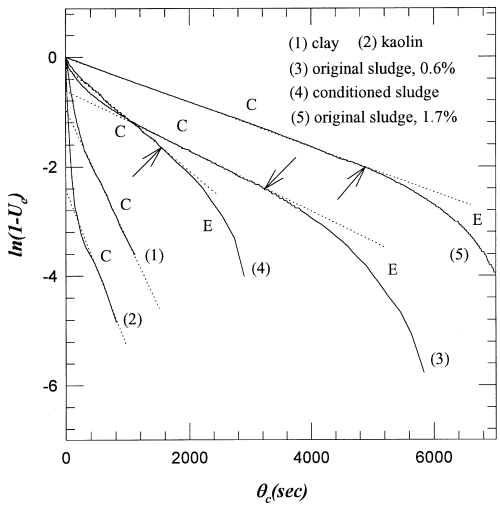

Fig. 2. $\ln(1 - U_c)$ versus θ_c plot. P = 1000 psi. C: consolidation period; E: final constant-rate period. Arrows indicate the transition of E region. Dashed lines are regression line based on equation (1).

As Fig. 2 illustrates, a linear $\ln(1-U_c)-\theta_c$ region appears after an initial decrease in U_c. This confirms the validity of employing equation 1 to describe the expression characteristics of the sludges employed in this work. Table 1 lists the best fitting coefficients B and η.

The B values for kaolin (0.082) and for clay (0.38) demonstrate a relatively strong primary consolidation period (92% and 62% respectively). The B value for the original activated sludge (0.55) is larger than those for particulate systems, indicating a relatively weaker primary consolidation for the former. It is also interesting to note that a physical conditioning such as freeze/thaw conditioning provides can destroy almost all primary consolidation, as observed by the close to unity B value (0.89).

The corresponding η values for activated sludge systems are much smaller than for the particulate systems. Therefore, the ease with which particle creeping occurs in the following sequence: kaolin (2) > clay(1) > conditioned sludge (4) > original sludge (3). The constituent particles in the original sludge cake exhibit a greater resistance to creeping motion. Restated, disturbing the bonding between particles is more difficult. Freeze/thaw conditioning, however, largely increases the mobility of the constituent particles.

Table 1 also listed the coefficient of consolidation, the *Ce* value, found by the fitting method proposed by Shirato *et al.* (1967). The smallest *Ce* value for the original sludge corresponds to the largest α_{av} value among these sludges. This value largely increases for the conditioned sludge, in response to a decrease in cake resistance (Lee and Hsu, 1994). For particulate systems, the *Ce* of kaolin slurry is greater than that of clay, reflecting less resistance to expression in the former.

In particulate tests, such as the clay and kaolin employed in this work, the expression reaches equilibrium after the region C. However, as Fig. 2 illustrates, for biological sludges, original or conditioned, a concave downward region exists after the linear $\ln(1-U_c)-\theta_c$ with a much higher (constant) filtrate flow rate than expected. Notably, Kawasaki *et al.* (1990, 1994) also illustrated in their Fig. 7 that the conventional combined Terzaghi-Voigt model predicts the expression process well till $U_c=0.8$. Above this consolidation ratio deviation between the model and experiment occurs. This final stage of expression is commonly observed in biosludges that had been examined in our lab.

We indicate this period by symbol E in Fig. 1. The arrows in Fig. 1 separating regions C and E, are located by deviations from the linear relationship in Fig. 2. If based on the total amount of moisture removal, there is a fraction of approximately 10% for the original and 30% for the conditioned sludges of the moisture expressed is attributed to region E. Since the primary and the secondary consolidations of expression of biological sludge can be described by the traditional combined Terzaghi-Voigt model, to take account of this final phase of expression, a modified version of the combined Terzaghi-Voigt model is employed in the subsequent sections. The expression equation is derived and solved analytically.

Model analysis

The mass balance of a liquid in an infinitesimal layer of cake at consolidation time θ_c can be stated as follows (Shirato *et al.*, 1977):

$$\frac{\partial e}{\partial \theta_c}=\frac{\partial u}{\partial \omega}, \tag{2}$$

where e, u are respectively the local void ratio and the apparent fluid velocity relative to solid. We propose here that the constant-rate period E can be described by the dynamics of a dashpot with a very large viscosity attaching to the combined Terzaghi-Voigt model (as demonstrated in Fig. 3). Therefore,

$$\left(\frac{\partial e}{\partial \theta_c}\right)=\left(\frac{\partial e}{\partial P_s}\right)_{\theta_c}\left(\frac{\partial P_s}{\partial \theta_c}\right)_{\omega}+\left(\frac{\partial e}{\partial \theta_c}\right)^{(2)}_{P_s}+\left(\frac{\partial e}{\partial \theta_c}\right)^{(3)}_{P_s} \tag{3}$$

The first, second and third terms of RHS of equation (3) represent respectively the primary, secondary and ternary consolidation stages.

Defining the coefficient of compressibility as $-(\partial e/\partial P_s)\theta_c=a_E(=(1+e)/E_1)$ (Shirato *et al.*, 1974), we have:

$$\left(\frac{\partial e}{\partial P_s}\right)_{\theta_c}\left(\frac{\partial P_s}{\partial \theta_c}\right)_{\omega}=-a_E\left(\frac{\partial P_s}{\partial \theta_c}\right), \tag{4}$$

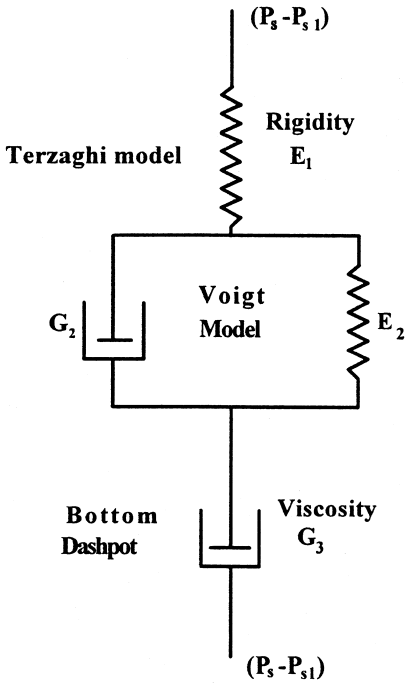

Fig. 3. Modified rheological model employed in the present work.

which accounts for the spring effect in the Terzaghi model. For the Voigt element, the following relation is noted (Shirato *et al.*, 1974):

$$\left(\frac{\partial e}{\partial \theta_c}\right)^{(2)}_{P_s} = \frac{\partial}{\partial \theta_c}\left[a_C \eta \int_0^{\theta_c} \{P_s(\omega,\tau) - P_{s1}\} \exp\{-\eta(\theta_c - \tau)\}\mathrm{d}\tau\right], \quad (5)$$

where $a_c = (1 + e)/E_2$, η the ratio E_2/G_2, P_s the local compressive pressure, and P_{si} the initial pressure distribution within the cake. Finally, the response of the bottom dashpot, whose coefficient of viscosity is G_3, is determined by the following equation:

$$G_3\left(\frac{\partial S_3}{\partial \theta_c}\right)_{\omega} = \{P_s(\omega,\theta_c) - P_{s1}\}, \quad (6)$$

where S_3 is the shear strain of the dashpot. With the initial condition $S_3 = 0$ at $\theta_c = 0$, the solution of equation 6 can be easily obtained as follows:

$$S_3(\theta_c) = \frac{1}{G_3}\int_0^{\theta_c} P_s(\omega,\tau)\mathrm{d}\tau - \frac{\theta_c P_{s1}}{G_3}. \quad (7)$$

With the help of the relation between the shear strain and the local void ratio, therefore, the following derivative is obtained.

$$\left(\frac{\partial e}{\partial \theta_c}\right)^{(3)}_{P_s} = -\frac{\partial}{\partial \theta_c}\left[a_G\left\{\int_0^{\theta_c} P_s(\omega,\tau)\mathrm{d}\tau - \theta_c P_{s1}\right\}\right], \quad (8)$$

where $a_G = (1 + e)/G_3$.

By combining equations (4), (5) and (8) into equation (2), employing the Ruth-Sperry equation and Leibnitz rule, the following partial differential equation results:

$$\frac{\partial P_s}{\partial \theta_c} + (\beta\eta + \gamma)P_s(\omega,\theta_c) - \beta\eta^2\int_0^{\theta_c} P_s(\omega,\tau)\exp\{-\eta(\theta_c - \tau)\}\mathrm{d}\tau - \{\beta\eta\exp(-\eta\theta_c) + \gamma\}P_{s1} = Ce\frac{\partial^2 P_s}{\partial \omega^2} \quad (9)$$

where $C_e = 1/\mu\rho_s\alpha_{av}\alpha_E$, α_{av} the average specific resistance of cake during consolidation, γ the ratio $a_G/a_E = E_1/G_3$, β the ratio $a_C/a_E = E_1/E_2$, and μ and ρ_s are filtrate viscosity and solid phase density, respectively. The initial and the boundary conditions are as follows:

$$P_s = P_{s1},\ 0 \le \omega \le \frac{\omega_0}{i},\ \theta_c = 0, \quad (10a)$$

$$P_s = P,\ \omega = 0,\ \theta_c > 0, \quad (10b)$$

$$\frac{\partial P_s}{\partial \omega} = 0,\ \omega = \frac{\omega_0}{i},\ \theta_c > 0 \quad (10c)$$

P is the applied pressure, i, number of drainage surface, and ω_0, the cake volume per unit area of filter surface.

Equation (9) with the conditions in equation (10) can be solved by Laplace Transform. The details and the associated parameters are given in the Appendix. The solution is as follows:

$$P_s(\omega,\theta_c) = P\left(1 - [D_{11}\exp(\lambda_{11}\theta_c) + D_{21}\exp(\lambda_{21}\theta_c)]\sin\left\{\frac{\pi}{2}\frac{i\omega}{\omega_0}\right\}\right) \quad (11)$$

Notably, the solution for P_s is in exactly the same form as that for traditional combined Terzaghi-Voigt model proposed by Shirato *et al.* (1974), except that the parameter γ is incorporated in the parameters λ_{11} and λ_{21} (and also D_{11} and D_{21}). Apparently, if γ is approaching zero, or equivalently the bottom dashpot is turned off, the solution for P_s reduces to that in Shirato *et al.* (1974).

The resulting cake thickness can therefore be obtained as follows:

$$\begin{aligned} L_1 - L &= \int_0^{\omega_0}(e_1 - e)\mathrm{d}\omega \\ &= \frac{2a_E P\omega_0}{\pi i}\{1 - D_{11}\exp(\lambda_{11}\theta_c) - D_{21}\exp(\lambda_{21}\theta_c)\} \\ &\quad + \frac{2a_C P\omega_0}{\pi i}\left\{1 + \left(\frac{\eta D_{11}}{\eta + \lambda_{11}} + \frac{\eta D_{21}}{\eta + \lambda_{21}} - 1\right)\exp(-\eta\theta_c) - \frac{\eta D_{11}}{\eta + \lambda_{11}}\exp(\lambda_{11}\theta_c) - \frac{\eta D_{21}}{\eta + \lambda_{11}}\exp(\lambda_{21}\theta_c)\right\} \\ &\quad + \frac{2a_G P\omega_0}{\pi}\left\{\theta_c - \frac{D_{11}}{\lambda_{11}}\exp(\lambda_{11}\theta_c) + \frac{D_{11}}{\lambda_{11}} - \frac{D_{21}}{\lambda_{21}}\exp(\lambda_{21}\theta_c) + \frac{D_{21}}{\lambda_{21}}\right\}. \end{aligned} \quad (12)$$

From Table 1, we observe that if $\pi^2/4\cdot i^2 Ce/\omega_0^2 \gg \eta$ (a much lesser rate for secondary consolidation than that for primary consolidation), and a very small γ (a relatively very viscous bottom dashpot), then $\lambda_{11} \to -\pi^2/4\cdot i^2 Ce/\omega_0^2$, $\lambda_{21} \to -\eta$, $D_{11} \to 1$, $D_{21} \to 0$, $\eta D_{11}/\eta + \lambda_{11} \to 0$ and $\eta D_{21}/\eta + \lambda_{21} \to 1$, the solution in equation (12) can be simplified as follows:

$$L_1 - L = \frac{2P\omega_0 a_E}{\pi i}\left[\left\{1 - \exp\left(-\frac{\pi^2 i^2 Ce}{4\omega_0^2}\theta_c\right)\right\} + \beta\{1 - \exp(-\eta\theta_c)\} + i\gamma\left\{\theta_c + \frac{4\omega_0^2}{\pi^2 i^2 Ce}\left(\exp\left(-\frac{\pi^2 i^2 Ce}{4\omega_0^2}\theta_c\right) - 1\right)\right\}\right]. \quad (13)$$

As consolidation time is large enough to make the exponential terms in equation (13) become negligible ($\pi^2 i^2 Ce/4\omega_0^2\theta_c \gg \eta\theta_c >$ say, 5), and noting the previously made assumption $\pi^2/4 \cdot i^2 Ce/\omega_0^2 \gg \eta$, equation (13) approaches the following linear relationship:

$$L_1 - L = \frac{2P\omega_0 a_E}{\pi i}[1 + \beta + i\gamma\theta_c]. \qquad (14)$$

That is, the cake thickness decreases with the consolidation time, as was found for the period E.

In practice the consolidation cannot last forever and will cease when all removable moisture has been forced out. A characteristic consolidation time θ_c^* can be defined to signal the end of the consolidation. Then the final thickness can be found as:

$$L_1 - L_f = \frac{2P\omega_0 a_E}{\pi i}[1 + \beta + i\gamma\theta_c^*]. \qquad (15)$$

Let $K = 1 + \beta + i\gamma\theta_c^*$, combine equation (13) and (15), resulting in the following relation for the consolidation ratio:

$$U_c = \frac{L_1 - L}{L_1 - L_f} = (1 - B - F)\left\{1 - \exp\left(-\frac{\pi^2 i^2 Ce}{4\omega_0^2}\theta_c\right)\right\} + B\{1 - \exp(-\eta\theta_c)\} + F\left\{\frac{\theta_c}{\theta_c^*} + \frac{4\omega_0^2}{\pi^2 i^2 Ce\theta_c^*}\left(\exp\left(-\frac{\pi^2 i^2 Ce}{4\omega_0^2}\theta_c\right) - 1\right)\right\}, \qquad (16)$$

where $B = \beta/K$ and $F = i\gamma\theta_c^*/\mathrm{K}$. The first and second brackets in equation (16) account for the primary and the secondary consolidation processes discussed in Shirato *et al.* (1974); while the third bracket is for the bottom dashpot. In the present work the second term in the last bracket is notably much smaller than the first term except at the commencement of consolidation. The ternary consolidation is therefore mainly determined as $U_3^{(3)} = F\theta_c/\theta_C^*$.

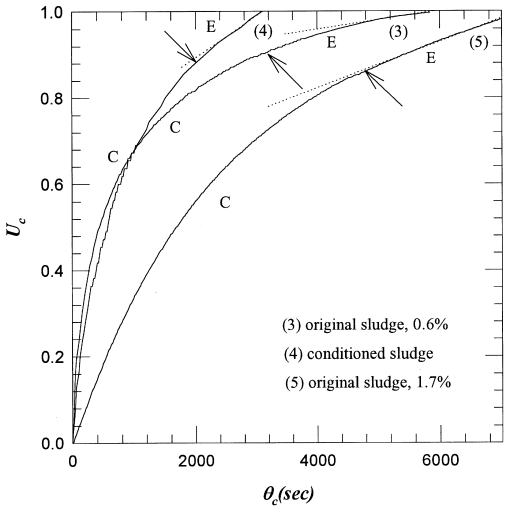

Fig. 4. U_c versus θ_c plot. P = 1000 psi. C: consolidation period; E: final constant-rate period. Arrows indicate the transition of E region. Dashed lines are regression line based on equation (18).

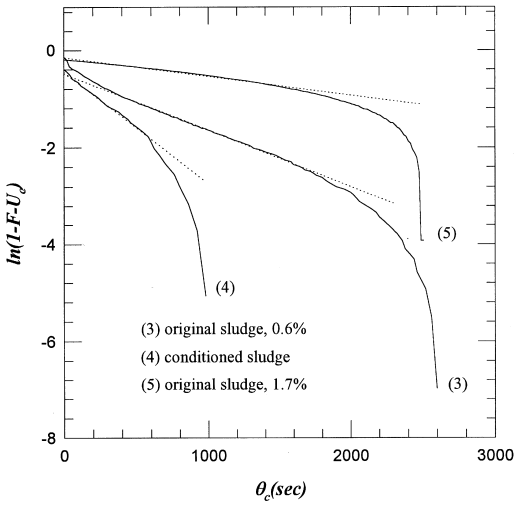

Fig. 5. $\ln(1 - F - U_c)$ versus θ_c plot. P = 1000 psi. C: consolidation period; E: final constant-rate period. Dashed lines are regression line based on equation (17).

During the intermediate stage where $\pi^2 i^2 Ce/4\omega_0^2\theta_c \gg 5 > \eta\theta_c$, equation (16) becomes

$$U_c = (1 - F) - B\exp(-\eta\theta_c), \qquad (17)$$

which will reduce to equation (1) if parameter F is much smaller than unity ($\gamma \to 0$). Under $\theta_c \to \infty$ limit, equation (16) becomes:

$$U_c = (1 - F) + \frac{F}{\theta_c^*}\theta_c, \qquad (18)$$

which is the final constant-rate consolidation period.

Parameter estimation of biological sludges

The procedures for parameter estimation are as follows. First, estimate the parameters F and θ_c^* from the final phase data in region E in Fig. 2 based on equation (18), as demonstrated in Fig. 4. The best fitted parameters are also listed in Table 1. Notably parameter F is not necessarily much smaller than unity, which places the corresponding B and η values estimated based on equation 1 in question.

The parameter F is then substituted into equation (17) to estimate corrected parameters B and η from the intermediate period of experimental data. Figure 5 depicts the $\ln(1 - F - U_c) - \theta_C$ plot. A satisfactory linearity is also observed for the intermediate period of the experimental data. The best-fitted B and η values are listed in Table 1. The newly found η values have doubled and acquired in the same order as those for kaolin and clay systems, indicating an underestimation of the creeping effect derived from equation 1. The change in B values is less significant.

Integration of equations (4), (5) and (8) with respect to consolidation time over the interval [0, θ_c^*] can yield a void ratio change during consolidation. The parameters B and F therefore represent respectively the fractions of moisture removed by secondary and ternary consolidation. The remaining fraction $1-B-F$, by definition, is contributed by primary consolidation.

The relative moisture removal for primary, secondary and ternary consolidation ($1-B-F$, B, F) are (0.29, 0.58, 0.13) for original sludge, (0.04, 0.64, 0.32) for conditioned sludge, (0.62, 0.38, 0) for clay slurry, and (0.92, 0.089, 0) for kaolin slurry. Primary consolidation is the major dewatering mechanism for particulate systems; with kaolin slurry (intermediate compressible) more than 90%, and with clay (highly compressible), 60% of moisture is moved. The corresponding percentage of moisture removed from original sludge is somewhat lower (30%), while freeze/thaw conditioning further reduces it to around 4%.

For the secondary consolidation, the percentage of moisture removal is 58% for original and 64% for conditioned sludges. This is contrary to the conclusion indicated by the parameters estimated by equation 1 stating that the value of B largely changes from 55% to 89% after conditioning. The ternary consolidation is 13% for original and 32% for conditioned sludges. At a first glance it seems strange for a conditioned sludge to exhibit a relatively larger contribution by ternary consolidation.

The total amount of moisture removal during the consolidation period are 11 g, 12.6 g, 36.8 g, and 5.5 g for clay, kaolin, original, and conditioned sludge, respectively. The amount (g) of moisture removal during first, second and ternary consolidation periods becomes (10.7, 21.3, 4.8) for original sludge, (0.22, 3.5, 1.8) for conditioned sludge, (6.8, 4.2, 0) for clay slurry, and (11.6, 1.0, 0) for kaolin slurry. It is clear, therefore, with freeze/thaw conditioning that the total moisture removal during all the three consolidation periods is greatly reduced. The relatively higher ternary consolidation for conditioned sludge is attributed to the even greater in decrease during both the primary and secondary consolidation periods.

From the obtained F and B values, the parameter β can be calculated. The value for original sludge is approximately 2, giving $E_1 = 2E_2$. Based on the parameters F and θ_c^*, the parameter γ can be also calculated and listed in Table 1. In kaolin and clay tests, no ternary consolidation period exists, while the corresponding γ values are by definition zero. For the original sludge, the parameter γ is of small value (8×10^{-5}), indicating a very large G_3 and confirming the previously assumed highly viscous dashpot. (Notably, η is 1.1×10^{-3}, thereby giving $G_3 = 25G_2$). Following freeze/thaw conditioning, the parameter γ largely increases, up to the same order of η, indicating a lowering of dashpot viscosity. The corresponding β value is about 15, therefore giving an $E_1 = 15E_2$. As a result, G_3 is now reduced to approximately $11G_2$ (a still much higher viscosity, nevertheless).

Although four parameters are involved in the rheological model (E_1, E_2, G_2, G_3), only three relative values are available (β, η, γ). Their relative importance can be found as follows. Take the spring rigidity E_1 as unity for various sludges as a reference. (Note: the E_1 for various sludge systems differs markedly. It is the relative significance between the other three parameters are of concern here.) The corresponding (E_2, G_2, G_3) are (0.5, 460, 12300) for original sludge, (0.066, 29.5, 333) for conditioned sludge, (1.7, 700, ∞) for clay slurry, and (11.2, 3970, ∞) for kaolin slurry. A comparison of the relative importance between model parameters, or the qualitatively rheological characteristics, indicates that the original sludge behaves somewhat like the clay slurry, which is a highly compressible material. The rigidity E_2 (viscosity G_2) of kaolin is much higher (lower) than that of other sludges, thereby giving a relatively faster (slower) primary consolidation (secondary consolidation). The conditioned sludge, on the other hand, exhibits behavior less similar to a particulate system than original sludge.

In some previous studies, in some respects, the freeze/thaw conditioned sludge is found to be more like a particulate system than a floc system, for example, the characteristics of free-settling (Lee *et al.*, 1996), zone settling (Chen, *et al.*, 1996b), floc structure (Lee, 1994a, Lee and Hsu, 1994) and the corresponding bound water content (Lee, 1994b, Lee and Lee, 1995, Chen *et al.*, 1997). In this study, the change in expression characteristics seems to lead to a contrary conclusion. Some interpretation will be attempted in the next section.

Ternary consolidation

Primary consolidation, it has been proposed, is dominated by the dissipation of excess pore water and the collapse of cake global structure. Most of the easily removed moisture, including some interstitial water among and within flocs, is removed during this stage. The secondary compression is usually interpreted as the constituent particles readjusting into a more stable configuration, the rate of which is mainly controlled by a highly viscous film of adsorbed water surrounding the surfaces of the constituent particles (Craig, 1993). Most interstitial water should be removed during this stage. The mechanism of the ternary consolidation, as identified in the present work, has not yet been fully investigated, a fact which merits some further discussion.

It might be of interest to examine the possible role of solid concentration in relation to activated sludge expression characteristics. The final sludge thickness of the original sludge is about 4 mm, while for freeze/thawed sludge it is about 2.5 mm. Another sample, a sediment of an activated sludge,

is tested to examine this point. Its solid concentration is 1.7% (w/w), about three times that of the activated sludge previously discussed. The expression data are depicted as curve #5 in Figs 1, 2, 4 and 5. The expression time lasts for four h, while the final consolidated cake thickness is 12.5 mm, indicating a larger amount of bound water contained in this sample. However, the basic characteristics are the same as the sludge with lower solid concentration. Its $(B,\eta,F) = (0.99, 0.00041, 0.36)$, reflecting a higher B and F, and a lower creeping factor. As a result, the solid concentration has generally not influenced the behavior of the consolidation process for activated sludge.

The pressure distribution can be approximately stated as follows:

$$P_s(\omega, \theta_c) = P\left(1 - \exp\left(-\frac{\pi^2 i^2 Ce}{4\omega_0^2}\theta_c\right)\sin\left\{\frac{\pi}{2}\frac{i\omega}{\omega_0}\right\}\right), \tag{19}$$

which approaches a uniform distribution of P over the whole cake as θ_c is large. That is, the pressure distribution within the cake changes mainly during primary and secondary consolidation, but remains constant in the ternary consolidation period. Accordingly, for ternary consolidation, the pressure-drop driven flow should not be the major dewatering mechanism. Neither is any serious particle migration (creeping) to be expected; this should largely be accomplished during the secondary consolidation period.

Owing to the nonexistence of a ternary consolidation period for the expression of particulate systems (clay and kaolin), the strong correlation between the parameter γ and the freeze/thaw conditioning (original and conditioned sludges), and to the comparatively very large coefficient of viscosity of the bottom dashpot (G_3), we hypothesize a possible mechanism corresponding to this stage of consolidation which involves deformation and compression of the constituent biological particles, accompanied with the erosion of adsorbed water on the surface of the particles or of the internal water within the biological materials. (Note: this erosion should occur all along the expression process and depend on the local compressive pressure that exerted. The rate of erosion becomes significant when both primary and secondary consolidation have accomplished, where the compressive pressure within the cake has reached a uniform, maximum value.) For sludges without a large amount of internal water, the role of a bound water erosion mechanism is negligible. For activated sludges, the binding strength between strongly bound moisture and the solid phase can range from several tens to several thousands kJ/kg (Lee and Lee, 1995), and the rate of erosion should be slow in giving a very high viscosity to the dashpot. The freeze/thaw conditioning will generate aggregates with a more compact structure and less internal water (Lee and Hsu, 1994), with which a cake with less interaggregate void volumes during filtration stage forms. No global structure change (and thereby almost no primary consolidation) occurs. Creeping of particles also becomes easier since the resulting particles are round-shaped and are less compressible (Lee and Hsu, 1994). During the ternary consolidation period, since the freeze/thaw conditioning largely weakens the binding strength between moisture and the solid phase (Lee and Lee, 1995), a lower G_3 and higher F values are observed. We can thereby conclude that the constituent particles are still more alike common particulate particles (less compressible, more compact structure, and less internal water). However, owing to the global cake structure created during the filtration stage is much tighter than that for the original sludge, the primary consolidation is almost invisible and makes the whole consolidation characteristics seem quite different from the particulate systems.

To sum up, the physical picture of expression of biological sludge is speculated as follows. When external pressure is applied to the sludge cake, the global cake structure formed during the filtration stage collapses accordingly and the (pore) interstitial water escapes with a rate controlled by Darcy's law. This stage is followed by a stage during which the constituent particles migrate to a more stable state. The motion of these particles requires to overcome the shear stress induced by the highly viscous, surface adsorbed water. The replacement will extrude more interstitial water and maybe some surface water. When all particles have attained their maximum stable states, the pressure distribution over the cake has become constant while the expression of common particulate systems reaches equilibrium. Nevertheless, for biological sludges with a large amount of internal water, there is a ternary consolidation period during which part of the strongly bound surface and internal water is released and forced out. The corresponding very large viscosity in the model parameters indicates the slow erosion rate of the moisture. For original sludge, the initial cake structure is loose and will collapse during primary consolidation. For the conditioned sludge, however, the initial cake structure is more compact which thereby removes primary consolidation.

The applicability of the present model should not consider confined to merely the original and freeze/thaw conditioned activated sludges discussed herein. Actually, we believed such a stage exists in other systems containing a large amount of bound water, such as polymer flocculated activated sludges. (Note: No such ternary expression stage is found for polymer flocculated, or alum coagulated clay slurries, in which not much bound water exists (Chang *et al.* 1997a,b).) Further research works are required to examine the applicability of the present model onto other sludges.

CONCLUSIONS

Expression characteristics of the original and freeze/thaw conditioned waste activated sludges were evaluated experimentally. Results in this study indicate that the primary and secondary consolidation periods of these biological sludges are similar to a particulate system, on which the combined Terzaghi-Voigt model analysis by Shirato *et al.* (1974) can be employed as a first approximation. Following these two periods, however, an unexpected constant-rate consolidation period is observed. A modified combined Terzaghi-Voigt rheological model is proposed to describe the void ratio-compressive pressure relation of the sludge cake, for which the governing equation is derived and solved analytically. Model parameters are evaluated by fitting the experimental data. A discussion on the relative rheological structure for various sludges during consolidation is made. The bound water erosion is speculated as the cause for the so-called ternary consolidation.

Acknowledgements—This work is supported by National Science Council, R.O.C.

REFERENCES

Chang I. L., Chu C. P., Lee D. J. and Huang C. (1997a) Effects of polymer dose on filtration followed by expression characteristics of clay slurries. *J. Colloid Interf. Sci.* **185,** 335–342.

Chang I. L., Chu C. P., Lee D. J. and Huang C. (1997b) Filtration followed by expression characteristics of alum coagulated clay slurry. *Environ. Sci. Technol.* in press.

Chen G. W., Lin W. W. and Lee D. J. (1996a) Use of capillary suction time (CST) as a measure for sludge dewaterability. *Wat. Sci. Tech.* **34,** 443–448.

Chen G. W., Chang I. L., Hung W. T. and Lee D. J. (1996b) Effects of freeze/thaw treatment on zone settling of waste activated sludge. *J. Environ. Sci. Hlth A*. **31,** 621–632.

Chen G. W., Chang I. L., Hung W. T., Lee S. F. and Lee D. J. (1997) Continuous classification of moisture in activated sludge. *J. Envir. Eng. ASCE* **123,** 253–258.

Craig R. F. (1993) *Soil Mechanics*, 5th Edn. Chap. 7. Chapman & Hall, London.

Drost-Hansen W. (1977) Effects of vicinal water on colloidal stability and sedimentation processes. *J. Colloid Interf. Sci.* **58,** 251–262.

Hung W. T., Chang I. L., Lin W. W. and Lee D. J. (1996) Unidirectional freezing of waste activated sludge: Effects of freezing speed. *Environ. Sci. Technol.* **30,** 2391–2396.

Katsiris N. and Kouzeli-Katsiri A. (1987) Bound water content of biological sludges in relation to filtration and dewatering. *Wat. Res.* **21,** 1319–1327.

Kawasaki K. and Matsuda A. (1993) Freezing and thawing of excess activated sludge to improve the solid liquid separation characteristics. *6th World Fil. Cong.*, Nagoya, Japan, pp. 865–868.

Kawasaki K., Matsuda A. and Murase T. (1990) The effects of freezing and thawing process on the expression characteristics and final moisture content of excess activated sludge. *Kagaku Kogaku Ronbunshu* **16,** 1241–1246.

Kawasaki K., Matsuda A. and Mizukawa Y. (1991) Compression characteristics of excess activated sludges treated by freeze-and-thawing process. *J. Chem. Engng. Japan*. **24,** 743–748.

Kawasaki K., Matsuda A. and Murase T. (1994) The effects of a freezing and thawing process on the expression characteristics and final moisture content of excess activated sludge. *Int. Chem. Engng* **34,** 403–409.

Lee D. J. (1994a) Floc structure and bound water contents in excess activated sludges. *J. Ch. I. Ch. E.* **25,** 201–207.

Lee D. J. (1994b) Measurement of bound water in excess activated sludges: Use of centrifugal settling method. *J. Chem. Tech. Biotechnol.* **61,** 139–144.

Lee D. J. and Hsu Y. H. (1994) Fast freeze/thaw process on excess activated sludges: Floc structure and sludge dewaterability. *Environ. Sci. Technol.* **28,** 1444–1449.

Lee D. J. and Hsu Y. H. (1995) Measurement of bound water in sludges. A comparative study. *Wat. Envir. Res.* **67,** 310–317.

Lee D. J. and Lee S. F. (1995) Measurement of bound water in sludges: Use of differential scanning calorimetry (DSC). *J. Chem. Tech. Biotechnol.* **62,** 359–364.

Lee D. J., Chen G. W., Liao Y. C. and Hsieh C. C. (1996) On the free-settling test for estimating waste activated sludge flocs. *Wat. Res.* **30,** 541–550.

Li D. H. and Ganczarczyk J. J. (1989) Fractal geometry of particle aggregates generated in water and wastewater treatment process. *Environ. Sci. Technol.* **23,** 1385–1389.

Li D. H. and Ganczarczyk J. J. (1990) Structure of activated sludge flocs. *Biotechnol. Bioengng* **35,** 57–65.

Michaels A. S. and Bolger J. C. (1962) Settling rates and sediment volumes of flocculated kaolin suspensions. *Ind. Engng Chem. Fundam.* **1,** 65–79.

Robinson J. and Knocke W. R. (1992) Use of diatometric and drying techniques for assessing dewatering characteristics. *Wat. Environ. Res.* **64,** 60–68.

Shirato M., Murase T., Hayashi N. and Fukushima T. (1977) Constant pressure expression of solid-liquid mixtures with medium resistance. *J. Chem. Engng Japan* **10,** 154–159.

Shirato M., Murase T., Kato H. and Fukaya S. (1967) Expression under constant pressure. *Kagaku Kogaku* **31,** 1125–1131 (in Japanese).

Shirato M., Murase T., Kato H. and Fukaya S. (1970) Fundamental analysis for expression under constant pressure. *Filtr. Sep.* **7,** 277–282.

Shirato M., Murase T., Kato H. and Shibata M. (1965) Analysis for constant pressure expression mechanism. *J. Fermentation Engng* **43,** 255–265 (in Japanese).

Shirato M., Murase T., Tokunaga A. and Yamada O. (1974) Calculations of consolidation period in expression operations. *J. Chem. Engng Japan* **7,** 229–231.

Shirato M., Murase T., Atsumi K., Aragaki T. and Noguchi T. (1979) Industrial expression equation for semi-solid materials of solid-liquid mixture under constant pressure. *J. Chem. Engng. Japan* **12,** 51–55.

Shirato M., Murase T., Atsumi K., Nagami T. and Suzuki H. (1978) Creep constants in expression of compressible solid-liquid mixtures. *J. Chem. Engng Japan* **11,** 334–336.

Tiller F. M. and Yeh C. S. (1987) The role of porosity in filtration. Part XI: Filtration followed by expression. *AIChE J.* **33,** 1241–1256.

Vesilind P. A. (1979) *Treatment and Disposal of Wastewater Sludges.* Ann Arbor Science, Ann Arbor, Mich.

Vesilind P. A. (1994) The role of water in sludge dewatering. *Wat. Environ. Res.* **66,** 4–11.

Yeh C. S. (1985) *Cake Deliquoring and Radial Filtration.* Doctoral Dissertation, University of Houston, Houston, Texas.

APPENDIX

Analytical solution of equation (9) in the text is given in this Appendix via Laplace transform. Only key equations are given for brevity sake.

Take Laplace transform of equation (9) on θ_c domain, with the help of initial condition equation (10a), leads to the following result:

$$\frac{\partial P_s}{\partial \omega^2} - A^2 P_s(\omega, s) + \frac{A^2}{s} P_{si}(\omega) = 0 \tag{A1}$$

where

$$A^2 = \frac{s^2 + s\eta + \beta s\eta + \gamma s + \gamma\eta}{Ce(\eta + s)}. \tag{A2}$$

The corresponding boundary conditions equation (10b) and (10c) had become:

$$P_s(0, s) = \frac{P}{s} \tag{A3}$$

$$\frac{\partial P_s\left(\frac{\omega_0}{i}, s\right)}{\partial \omega} = 0 \tag{A4}$$

The solution of equation (A1) with conditions equations (A2) and (A3) can be found as follows:

$$P_s(\omega, s) = \frac{P}{s}\cosh(A\omega) + \frac{1}{A}\sinh(A\omega)\frac{\partial P_s(0, s)}{\partial \omega} - \frac{A}{s}\int_0^{\omega} P_{si}(\xi)\sinh\{A(\omega - \xi)\mathrm{d}\xi. \tag{A5}$$

With the help of equation (A4), equation (A5) can be further reduced into:

$$P_s(\omega, s) = \frac{1}{s \cdot \cosh\left(\frac{A\omega_0}{i}\right)}\left[P \cdot \cosh\left\{\frac{A\omega_0}{i}\left(1 - \frac{i\omega}{\omega_0}\right)\right\} + A\int_0^{\frac{\omega_0}{i}} P_{si}(\xi)\sinh(A\omega)\cosh\left\{\frac{A\omega_0}{i}\left(1 - \frac{i\xi}{\omega_0}\right)\right\}\mathrm{d}\xi - A\int_0^{\omega} P_{si}(\xi)\cosh\left(\frac{A\omega_0}{i}\right)\sinh\{A(\omega - \xi)\}\mathrm{d}\xi\right]. \tag{A6}$$

The solution on θ_c domain can be found via inverse Laplace transform as follows:

$$P_s(\omega, \theta_c) = \sum_{n=1}^{\infty} \frac{r(s_n)}{q'(s_n)}\exp(s_n\theta_c) \tag{A7}$$

where

$$r(s) = P\cosh\left\{\frac{A\omega_0}{i}\left(1 - \frac{i\omega}{\omega_0}\right)\right\} + A\int_0^{\omega} P_{si}(\xi)\sinh(A\xi)\cosh\left\{\frac{A\omega_0}{i}\left(1 - \frac{i\omega}{\omega_0}\right)\right\}\mathrm{d}\xi + A\int_{\omega}^{\frac{\omega_0}{i}} P_{si}(\xi)\sinh(A\omega)\cosh\left\{\frac{A\omega_0}{i}\left(1 - \frac{i\xi}{\omega_0}\right)\right\}\mathrm{d}\xi \tag{A8}$$

and

$$q(s) = s\cosh\left(\frac{A\omega_0}{i}\right) \tag{A9}$$

s is the solution putting $q(s) = 0$, thereby giving:

$$s_0 = 0 \tag{A10}$$

$$s_n = -\lambda_{1n}, -\lambda_{2n}, \quad n = 1, 2, \ldots \tag{A11}$$

where

$$\{\lambda_{1n}, \lambda_{2n}\} = -\frac{1}{2}\left(\eta + \beta\eta + \gamma + \frac{(2n-1)^2\pi^2 i^2 Ce}{4\omega_0^2}\right) \pm \frac{1}{2}\sqrt{\left\{\eta + \beta\eta + \gamma + \frac{(2n-1)^2\pi^2 i^2 Ce}{4\omega_0^2}\right\}^2 - 4\left\{\gamma\eta + \frac{\eta(2n-1)^2\pi^2 i^2 Ce}{4\omega_0^2}\right\}} \tag{A12}$$

The solution of P_s becomes:

$$P_s(\omega, \theta_c) = P - \sum_{n=1}^{\infty}\left[\frac{4P}{(2n-1)\pi} - \frac{2i}{\omega_0}\int_0^{\omega_0/i} P_{si}(\xi)\sin\left\{\frac{(2n-1)\pi}{2}\frac{i\xi}{\omega_0}\right\}\mathrm{d}\xi\right] \times \{D_{1n}\exp(-\lambda_{1n}c) + D_{2n}\exp(-\lambda_{2n}\theta_c)\} \sin\left\{\frac{(2n-1)\pi}{2}\frac{i\omega}{\omega_0}\right\} \tag{A13}$$

where

$$D_{1n} = \frac{(\lambda_{1n} - \eta)^2}{\lambda_{1n}\{(\lambda_{1n} - \eta)^2 + \beta\eta^2\}} \cdot \frac{(2n-1)^2\pi^2}{4} \cdot \frac{i^2 Ce}{\omega_0^2} \tag{A14}$$

$$D_{2n} = \frac{(\lambda_{2n} - \eta)^2}{\lambda_{2n}\{(\lambda_{2n} - \eta)^2 + \beta\eta^2\}} \cdot \frac{(2n-1)^2\pi^2}{4} \cdot \frac{i^2 Ce}{\omega_0^2} \tag{A15}$$

Shirato *et al.* (1974) had adopted a sine form of initial pressure distribution where $P_{s1} = P\{1 - \sin(\pi/2 \cdot \mathrm{i}\omega/\omega_0)\}$, equation 13 can thereby be rearranged into the following form:

$$P_s(\omega, \theta_c) = P\left(1 - \sum_{n=1}^{\infty}[D_{1n}\exp(\lambda_{1n}\theta_c) + D_{2n}\exp(\lambda_{2n}\theta_c)]\sin\left\{\frac{(2n-1)\pi}{2}\frac{i\omega}{\omega_0}\right\}\right) \tag{A16}$$

Notably all λ s are negative and the magnitudes of their absolute values grow fast with increase in n. Take only $n = 1$ terms can describe system dynamics well except at the very beginning of an expression test, which gives equation 11 in the text.